

Influence of Processing Method on the Exfoliation Process for Organically Modified Clay Systems. I. Polyurethanes

Ian Rhoney, Steven Brown, Nicholas E. Hudson, Richard A. Pethrick

Department of Pure and Applied Chemistry, University of Strathclyde, Thomas Graham Building, 295 Cathedral Street, Glasgow G1 1XL, Scotland

Received 14 February 2002; accepted 28 March 2003

ABSTRACT: The influence of different processing methods on the nature of the dispersion achieved in the creation of a polyurethane nanocomposite is presented. The nanocomposites were produced using two different types of organically modified montmorillonite clays and a sample of fine particles of silicon nitride as a reference material. Rheological data were used to assess the nature of the dispersion achieved using the different processing methods. The nature of the dispersion produced was characterized using wide-

angle X-ray scattering measurements of the finally cured products. Dynamic mechanical thermal analysis was used to investigate the effect of the incorporation of clay platelets into the matrix of the polymer. The high-temperature modulus provides evidence of the interaction between the polymer and the clay platelets; however, surprisingly, the glass transition temperatures of the filled and unfilled materials were almost identical. © 2003 Wiley Periodicals, Inc. *J Appl Polym Sci* 91: 1335–1343, 2004

INTRODUCTION

The potential of producing materials with enhanced physical properties by the incorporation of clay particles into polymer matrixes has been amply demonstrated in the literature.^{1–5} A careful examination of the published data, however, reveals that the nature of the clay dispersion upon which the enhanced physical properties are based is not always well defined. Depending on the interaction between the layered silicate platelets and the organic species present, intercalation is achieved via either insertion of a suitable monomer and subsequent polymerization or direct insertion of a polymer chain from a solution or a melt.³ To achieve the optimum enhancement of the physical properties, exfoliation of the platelets is the desirable objective of the dispersion processes.^{6–8} Many of the studies reported use organically modified materials as precursors, and the intercalated materials obtained often appear to have distances which are only slightly larger than those observed for the original organic-modified material. The interlayer expansion in exfoliated nanocomposites should exceed the separation associated with the organic modification and the platelets should also lose their structural registry.⁹ From the processing point of view, the mechanical and rheological properties of these nanocomposites are of great interest.¹⁰

There are few studies of the rheology of nanocomposite systems in which the influence of the dispersion method on the viscosity behavior has been reported. Among the various clay minerals, layered smectic-type montmorillonite (MMT) clay has been widely used to create nanocomposites. MMT, a hydrous alumina silicate mineral whose lamellae are constructed from octahedral alumina sheets sandwiched between tetrahedral silicate sheets, exhibits a net negative charge on the lamellar surface, when aluminum is substituted by magnesium or iron atoms.¹¹ The anionic character of the surface sites allows absorption of Na⁺ or Ca²⁺. A number of organically modified alkyl ammonium cations are now available to aid the dispersion of individual platelets into the reaction mixture. The platelets will also naturally absorb water molecules unless the organic modification is sufficiently large to block hydrogen bonding with the surface silicone–oxygen bonds.

In this article, the effect of a number of different dispersion methods on the nature of the initial reactive liquid media and the reaction product are reported. Three different processing methods were investigated:

- First, a Heidolph high-speed stirrer of the type usually used for the creation of emulsions was examined. The Heidolph mixer used a spiked, baffled mixing head with a rotational speed of 5000 rpm.
- Second, a high-shear Ultra-Turrax T25 mixer (usually used to create colloidal dispersion of fine particles) was used. This has a rotational speed of 24,000 rpm.

Correspondence to: N. E. Hudson.
Contract grant sponsor: EPSRC.

- Third, sonication of the liquid was examined using a Soniprobe fitted with a 5-mm-diameter truncated probe, while the fluid was stirred at 300 rpm. This technique is commonly employed when both high speed and high shear are required to create colloidal dispersions of fine particles or to destroy biological cells.

The methods of dispersion were compared through rheological measurements and X-ray diffraction analysis of the products of the polymerization process. As a reference system, fine particles of silicon nitride were also studied. These particles cannot undergo fragmentation and are insensitive to water.

EXPERIMENTAL

Materials

Two organically modified mica-type silicates (OMTS, supplied by Southern Clay Products, Gonzales, TX) were used in the preparation of the nanocomposites. The clays used in this study were intercalated using either bis(2-hydroxyethyl)methyl tallow (predominantly C-18 hydrocarbon) ammonium montmorillonite (140 meq/100 g; Cloisite 30B) or dimethyldihydrogenated tallow (predominantly C-18 hydrocarbon) ammonium montmorillonite (92 meq/100 g; Cloisite 6A). The polyurethane-cast elastomers were produced using the reaction of a mixture of difunctional poly(propylene glycol) (PPG; M_w 425, Aldrich) as the soft segment and 1,3-propane diol (Aldrich) as the chain extender with polymeric methylenediphenylisocyanate (MDI; functionality ~ 2.5 ; Suprasec 5005, Huntsman Chemical Co.) as the reactive isocyanate. Silicon nitride (Si_3N_4) was obtained from Aldrich as a fine powder with a mean particle size of ~ 5 – 10 microns.

Cure of the polyurethanes

The isocyanate, chain-extender, and PPG were dried using vacuum-distillation. The reagent was placed, with a magnetic stirrer, in a 250-mL round-bottomed flask attached to a vacuum line and distillation was achieved by immersion in a water bath heated to 50°C using an electric stirring hot plate. The clays used are very low density and tended to float on top of the liquid polyol. A slow-speed mixing was used to initially disperse the clay in the liquid. The dispersion was then subjected to stirring with a Heidolph mixer, an Ultra Turrax High shear mixer, or sonication using a high-energy biological cell destruction probe. The dry isocyanate was added in the correct amounts to the polyol blend and the mixture stirred for 2 min before further degassing. During the degassing procedure, a magnetic stirring bar was added to the blend

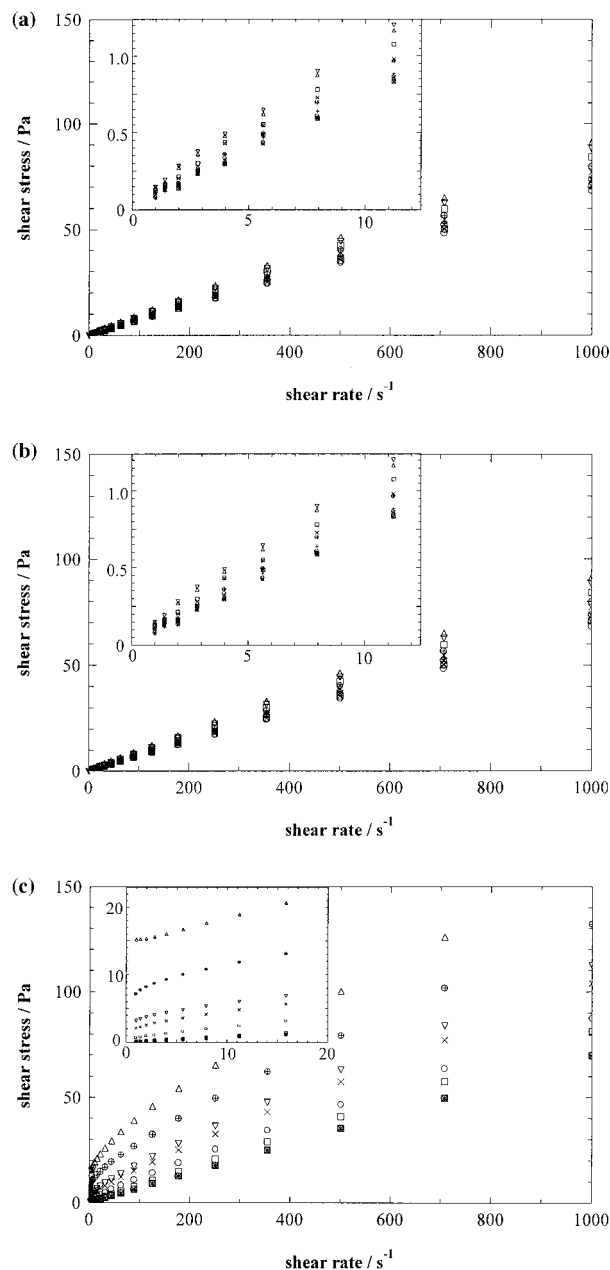


Figure 1 Controlled shear rate tests. Shear stress against shear rate for polyol with clay: (a) Heidolph mixer for 15 min; (b) Ultra Turrax high shear mixer for 15 min; (c) sonication for 15 min. A_n , $n\%$ of Cloisite 6A; B_n , $n\%$ of Cloisite 30B; SN_n , $n\%$ of Si_3N_4 . (\circ) A1; (\square) A2; (∇) A3; (\times) B1; (\oplus) B2; (\triangle) B3; ($+$) SN1; (\otimes) SN2; (\boxtimes) SN3.

and the container placed inside an airtight vessel on top of a magnetic stirrer plate. As a vacuum was applied, the stirrer helped to agitate the system and release the gas. The mixture was left to degas for as long as the cure time would allow (between 15 and 20 min). The polyurethane blend, now a viscous fluid, was poured into a suitable mold and allowed to cure. The polyurethane was cured at 90°C in an oven for 16 h.

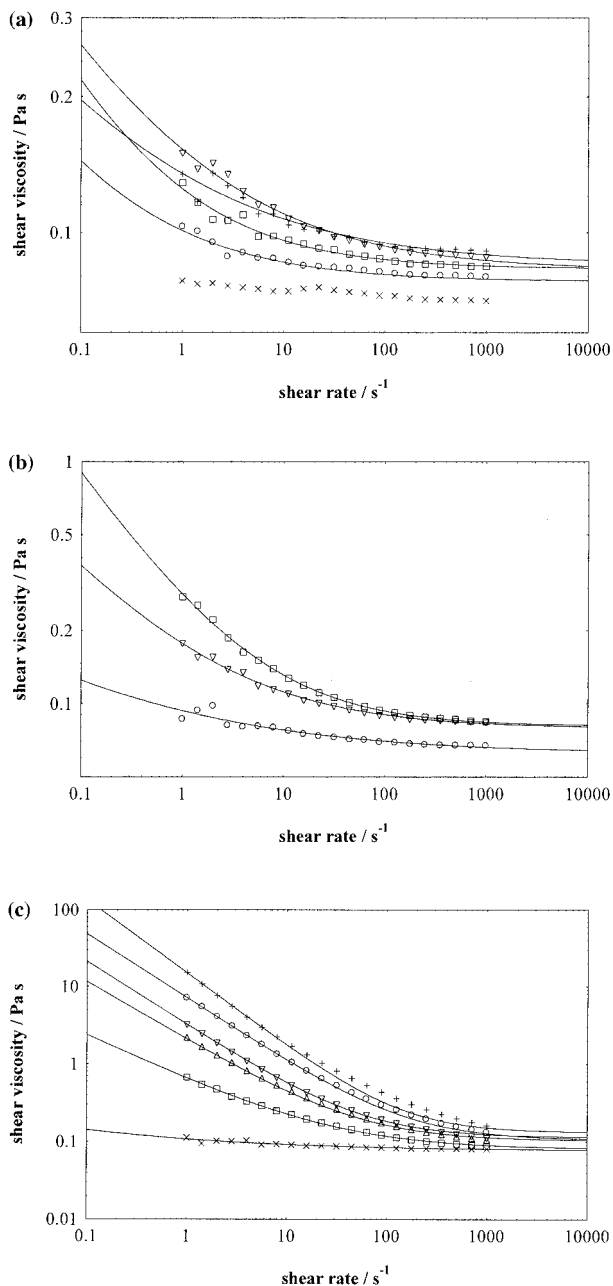


Figure 2 Controlled shear rate tests. Shear viscosity against shear rate for polyol with clay. (a) Heidolph mixer for 15 min: (×) SN3; (□) A2; (▽) A3; (○) B2; (+) B3. (b) Ultra Turrax high shear mixer for 15 min: (○) B1; (▽) B2; (□) B3. (c) Sonication for 15 min; (×) A1; (□) A2; (▽) A3; (△) B1; (○) B2; (+) B3. The lines are Sisko model fits. Parameters are shown in Table I.

Analytical methods

X-ray diffraction (XRD) measurements

A Siemens D500 X-ray diffractometer with a CuK α ($\lambda = 1.54 \text{ \AA}$) radiation source and a curved graphite crystal monochromator was used to analyze the samples. XRD experiments were performed directly on the OMTS powders and on OMTS/polyurethane.

Dynamic mechanical thermal analysis (DMTA) measurement

A Polymer Laboratories MKIII dynamic thermal analysis instrument operating at a frequency of 1 Hz and a temperature scanning rate of 3°C/min was used to characterize the samples produced. The measurements were performed using a two-point bending configuration.

Rheological measurements

The rheological properties of the nanocomposite mixtures were examined using a CSL² 500 rheometer (TA Instruments, Leatherhead). The measuring system employed was a 20-mm-diameter parallel plate, and the gap between this plate and the Peltier plate was set to 250 μm . Tests were performed using a controlled shear rate (1–1000 s^{-1}) or controlled stress (1–100 Pa, held at 100 Pa for 2 min, then 100–1 Pa).

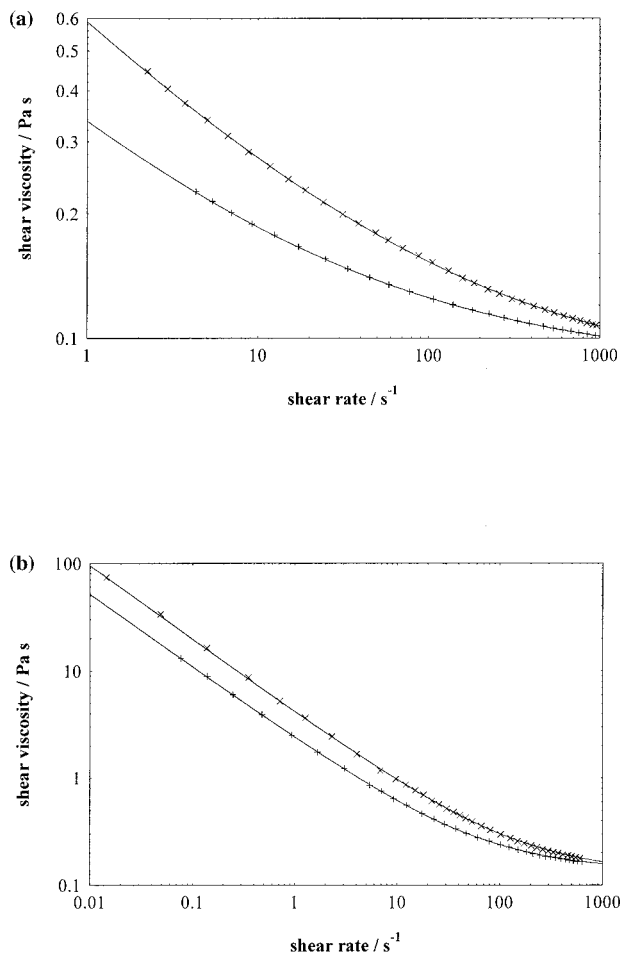


Figure 3 Controlled shear stress tests (1–100 Pa followed by 100–1 Pa). Shear viscosity at (×) an increasing shear rate and (○) a decreasing shear rate for (a) 2% Cloisite 6A and (b) 2% Cloisite 30B. The lines are Sisko model fits. Parameters are shown in Table I.

TABLE I
Analysis of the Viscosity Data Using the Sisko Equation

| System | Dispersion | η_{∞} (Pa s) | λ (s) | $1 - \eta$ |
|--------------|------------|------------------------|-------------------|---------------|
| Heidolph | A2 | 0.083 | 3.79 | 0.510 |
| | A3 | 0.083 | 1.56 | 0.406 |
| | B2 | 0.078 | 14.4 | 0.458 |
| | B3 | 0.085 | 4.63 | 0.349 |
| Ultra-Turrax | B1 | 0.063 | 11.5 | 0.300 |
| | B2 | 0.080 | 0.678 | 0.480 |
| | B3 | 0.081 | 0.221 | 0.608 |
| Soniprobe | A1 | 0.067 ± 0.008 | 20.48 | 0.177 ± 0.092 |
| | A2 | 0.078 ± 0.015 | 0.0327 ± 0.0041 | 0.589 ± 0.124 |
| | A3 | 0.114 ± 0.018 | 0.0182 ± 0.0078 | 0.828 ± 0.146 |
| | B1 | 0.090 ± 0.012 | 0.0153 ± 0.0039 | 0.743 ± 0.058 |
| | B2 | 0.114 ± 0.028 | 0.00699 ± 0.00252 | 0.832 ± 0.099 |
| | B3 | 0.150 ± 0.043 | 0.00853 ± 0.00348 | 0.965 ± 0.104 |
| | A1 up | 0.067 ± 0.007 | 0.00759 ± 0.00403 | 0.294 ± 0.086 |
| | A1 down | 0.070 ± 0.009 | 0.0299 ± 0.0078 | 0.316 ± 0.093 |
| | A2 up | 0.078 ± 0.013 | 0.0109 ± 0.0072 | 0.416 ± 0.113 |
| | A2 down | 0.085 ± 0.014 | 0.0651 ± 0.0124 | 0.398 ± 0.101 |
| | A3 up | 0.112 ± 0.016 | 0.00234 ± 0.00893 | 0.727 ± 0.153 |
| | A3 down | 0.118 ± 0.018 | 0.00682 ± 0.01413 | 0.736 ± 0.157 |
| | B1 up | 0.099 ± 0.011 | 0.0455 ± 0.0081 | 0.800 ± 0.067 |
| | B1 down | 0.098 ± 0.012 | 0.0590 ± 0.0168 | 0.728 ± 0.061 |
| | B2 up | 0.128 ± 0.018 | 0.00628 ± 0.00181 | 0.683 ± 0.114 |
| | B2 down | 0.136 ± 0.021 | 0.0152 ± 0.0062 | 0.675 ± 0.101 |
| | B3 up | 0.206 ± 0.039 | 0.00464 ± 0.00154 | 0.857 ± 0.098 |
| | B3 down | 0.218 ± 0.048 | 0.00783 ± 0.00238 | 0.845 ± 0.116 |

RESULTS AND DISCUSSION

Rheological measurements

A small number of publications have appeared recently on the rheological characterization of clay nanocomposites.^{5,10,13} It was observed¹⁰ that the viscosity increases substantially with an increased clay content at low shear rates and increases monotonically with clay loading at a given shear rate. This enhancement arises due to the interaction between the clay platelets in the polymer. Unlike a typical polymer, which exhibits a Newtonian plateau region at low shear rates, the intercalated nanocomposites have a yield stress followed by shear-thinning behavior. At high shear rates, the nanocomposites exhibit rapid shear thinning compared with the behavior of the polymer system in which they are dispersed. It has, however, been established that the enhancement of the rheological properties is closely correlated with a good dispersion of the platelets having been achieved.

The dispersions studied were coded as follows: Ax contains $x\%$ (w/w) Cloisite 6A, while By contains $y\%$ (w/w) Cloisite 30B. The initial study was performed on dispersions of the various loadings of clay dispersed in low molar mass polyol using the three mixing methods identified above. Examination of the shear stress versus shear rate data (Fig. 1) indicates that there is evidence of yield stress behavior only in the case of the well-dispersed sonicated material. The dis-

persions produced using the lower-energy methods show virtually no evidence for yield stress behavior (see insets). Neither the Heidolph nor Ultra Turrax high-shear mixer appeared to be able to achieve exfoliation of the clay; however, a relatively brief exposure to sonication immediately produces a stable dispersion. The dispersion with either the Heidolph or the Ultra Turrax high-shear mixer was inherently unstable and precipitation of clay would occur over a period of 1 day or more. The sonicated samples produced dispersions that were stable for weeks or more. The sonication process appears not only able to achieve a better but also a more stable dispersion. These data indicate that it is only when the polyol-clay mixture is sonicated does a major enhancement of the viscosity characteristics of the exfoliation of the OMTS occur. The Si_3N_4 particles have no interaction with the polymer and their dispersion is not influenced by the technique used, and, as expected, they only show a slight enhancement in the viscosity, as would be predicted by a simple Einstein particulate-loading model.

The data in Figure 1(a-c) were used to calculate the shear viscosity against the shear rate in Figure 2(a-c). The viscosity plots in the case of the sonicated material demonstrate the dramatic shear thinning observed by other workers.¹⁰ For these sonicated samples, the data obtained from the controlled shear stress trials are shown in Figure 3. The generic equation for shear flow of a polymer system is $\eta(\dot{\gamma}) = \eta_{\infty} + (\eta_0$

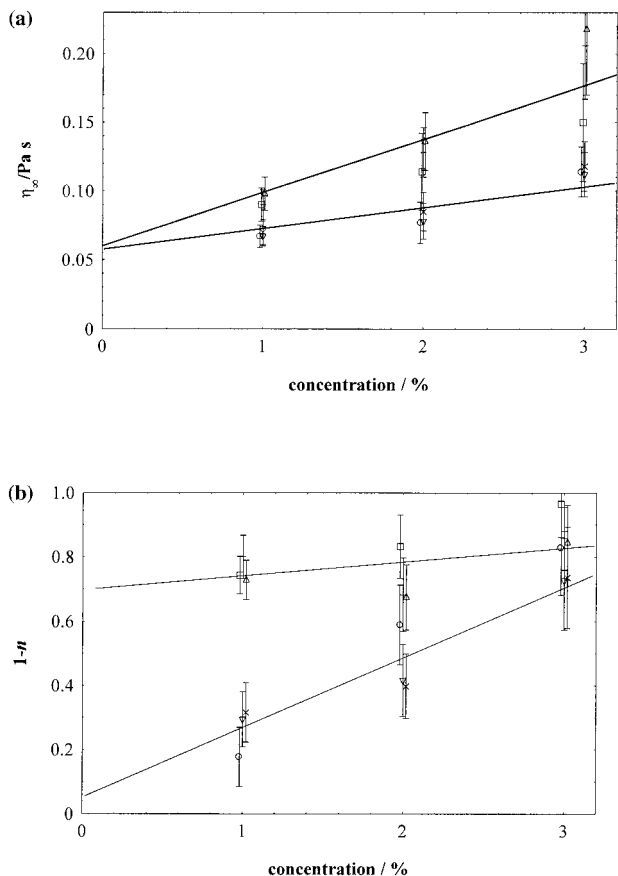


Figure 4 Sisko model parameters as functions of concentration: (a) high shear rate viscosity, η_{∞} and (b) power-law index, $1 - n$. Closite 6A: (○) controlled rate; (▽) controlled stress up; (×) controlled stress down. Closite 30B: (□) controlled rate; (×) controlled stress up; (△) controlled stress down.

– $\eta_{\infty}f(\dot{\gamma})$, where the function, $f\dot{\gamma}$, of the shear rate, $\dot{\gamma}$, satisfies the constraints $f(0) = 1$; $f(\infty) = 0$. One such function is

$$f(\dot{\gamma}) = \frac{1}{1 + (K\dot{\gamma})^m}$$

This gives rise to the Cross model equation,¹⁴

$$\eta(\dot{\gamma}) = \eta_{\infty} + \frac{(\eta_0 - \eta_{\infty})}{1 + (K\dot{\gamma})^m}$$

When $\eta \ll \eta_0$ and $\eta \gg \eta_{\infty}$, the Cross model can, in turn, be reduced to

$$\eta(\dot{\gamma}) = \frac{\eta_0}{(K\dot{\gamma})^m}$$

and by a simple redefinition of parameters, this equation can be written as the power-law model,¹⁴ $\eta(\dot{\gamma}) = K_2\dot{\gamma}^{n-1}$. n is called the power-law index, and K_2 is the “consistency.” If $\eta \ll \eta_0$, we have

$$\eta(\dot{\gamma}) = \eta_{\infty} + \frac{\eta_0}{(K\dot{\gamma})^m}$$

again being rewritten as the Sisko model,¹⁴ $\eta(\dot{\gamma}) = \eta_{\infty} + K_2\dot{\gamma}^{n-1}$. The viscosity data were therefore fitted to this Sisko equation. Since K_2 has the strange unit of Pa s^n , we can reform the equation into $\eta(\dot{\gamma}) = \eta_{\infty}[1 + (\lambda\dot{\gamma})^{n-1}]$. The fitting parameters obtained from the analysis are summarized in Table I. The base viscosity, η_{∞} , depends only on the viscosity of the fluid in which the clay platelets are dispersed [see Fig. 4(a)]. The

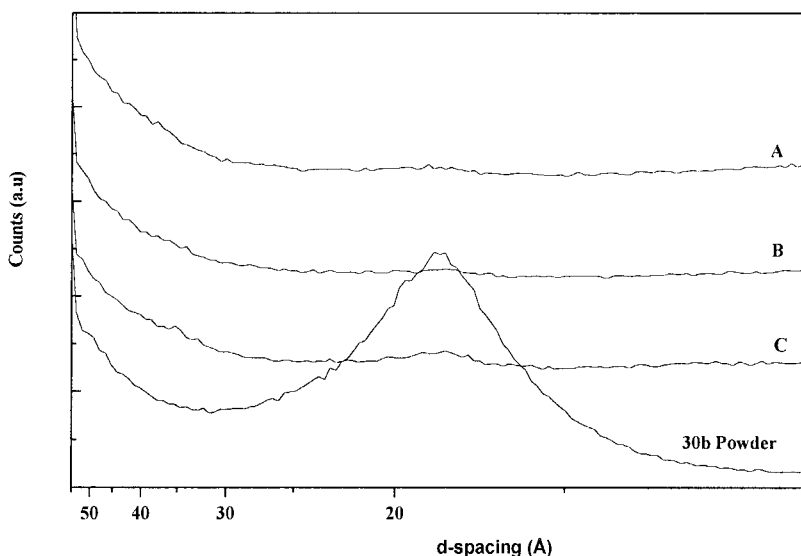


Figure 5 XRD spectrum of Closite 30B powder and cured OMTS/polyurethane-cured mixture: (A) 1.0% Closite 30b; (B) 2.0% Closite 30B; (C) 3.0% Closite 30B. Sample prepared by sonication.

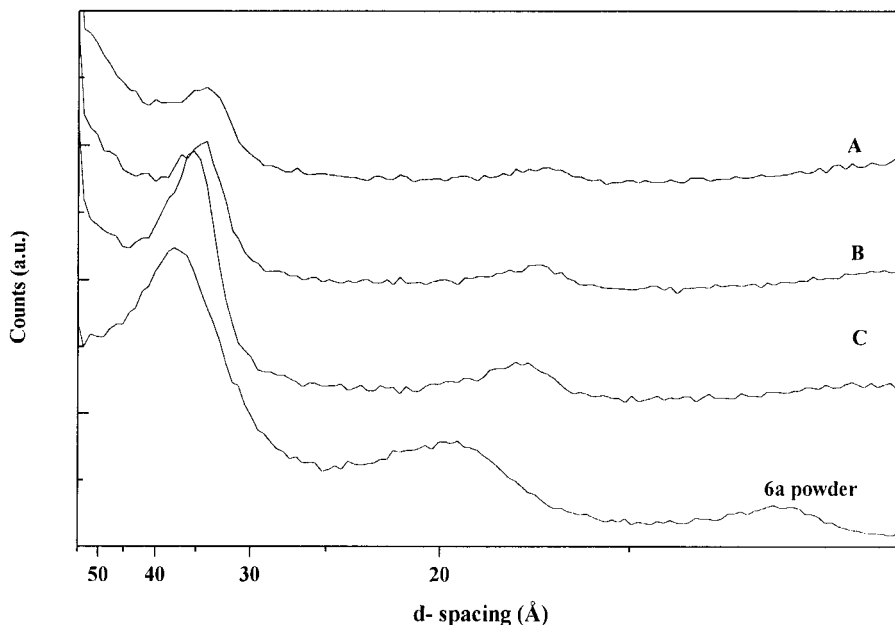


Figure 6 XRD spectrum of Cloisite 6A powder and cured OMTS/polyurethane-cured mixture: (A) 1.0% Cloisite 6A; (B) 2.0% Cloisite 6A; (C) 3.0% Cloisite 6A. Samples prepared by sonication.

concentration dependence of the relationship scales with the solid content as predicted by an Einstein-like relationship, $\eta = \eta_s(1 + [\eta]c)$, where $[\eta]$, the intrinsic viscosity, is a measure of the shape of the particle. The power-law index, n , is a reflection of the amount of entanglement in the system [see Fig. 4(b)], and a value of $n = 1$ means Newtonian behavior.

The differences between the up and down curves (Fig. 3) can be taken as an indication of the interactions between the platelets probably associated with a combination of the occurrence of edge-to-face interactions, which are lost when shearing of the platelets occurs, and interaction of the organic modifiers. If the shear rate/stress is small, then the rate of buildup under Brownian motion, etc., will match the breakdown, and the viscosity level will remain constant (i.e., Newtonian flow). As the shear rate/stress increases, the breakdown of the structure will occur at a faster rate than will the buildup, so shear thinning is seen. The breakdown rate usually depends upon the level of the structure, so viscosity levels are quite high on the up curve. When shearing decreases (the down curve), the breakdown of the structure will still occur at a faster rate than that of the buildup (but will now depend on a lower level of the structure), so the viscosity level will be less than that seen on the up curve.

The structure in these systems can be associated also with the interaction of the positive charges on the edge of the platelets with the negative charges in the surface of the platelets. These interactions will be reduced by shear, and together with the rotation of the platelets in the flow lines, are responsible for the rate dependence of the viscosity. The effect of the organic

modifiers is evident through a comparison of Cloisite 30B with Cloisite 6A, at 2% concentration, in Figure 3. In the former [Fig. 3(b)], the organic modifier has a single long chain and the difference between the up and down curves is small, but the viscosity is high. In the case of the Cloisite 6A [Fig. 3(a)], this has a stabilizer with two long chains, and there is a significant difference between the up and down curves, although the viscosity level is lower than that for Cloisite 30B.

The differences between the two organic modifiers is seen in Figure 4, where two of the Sisko model parameters are shown as functions of the concentration. Within the measurement and curve-fitting errors, the high shear rate viscosity [Fig. 4(a)] scales as $\eta_{\infty} = 0.575(1 + 26c)$ for Cloisite 6A and $\eta_{\infty} = 0.597(1 + 65c)$ for Cloisite 30B. Also, high concentrations of Cloisite 6A are needed to obtain the degree of non-Newtonian behavior seen with Cloisite 30B.

Characterization of the polyurethanes

XRD characterization of the dispersion

The samples obtained from the polymerization of the sonicated dispersion of clay in the polyol were examined using XRD [Figs. 4 and 5]. Cloisite 30B contains two ethanolic side groups on the chains of the cation. These hydroxyl groups are able to interact with the surface of the clay platelets and are also reactive with the diisocyanate, aiding the dispersion process. Cloisite 6A, however, has no such hydroxyl functions and, for that reason, is termed "unreactive." In the case of

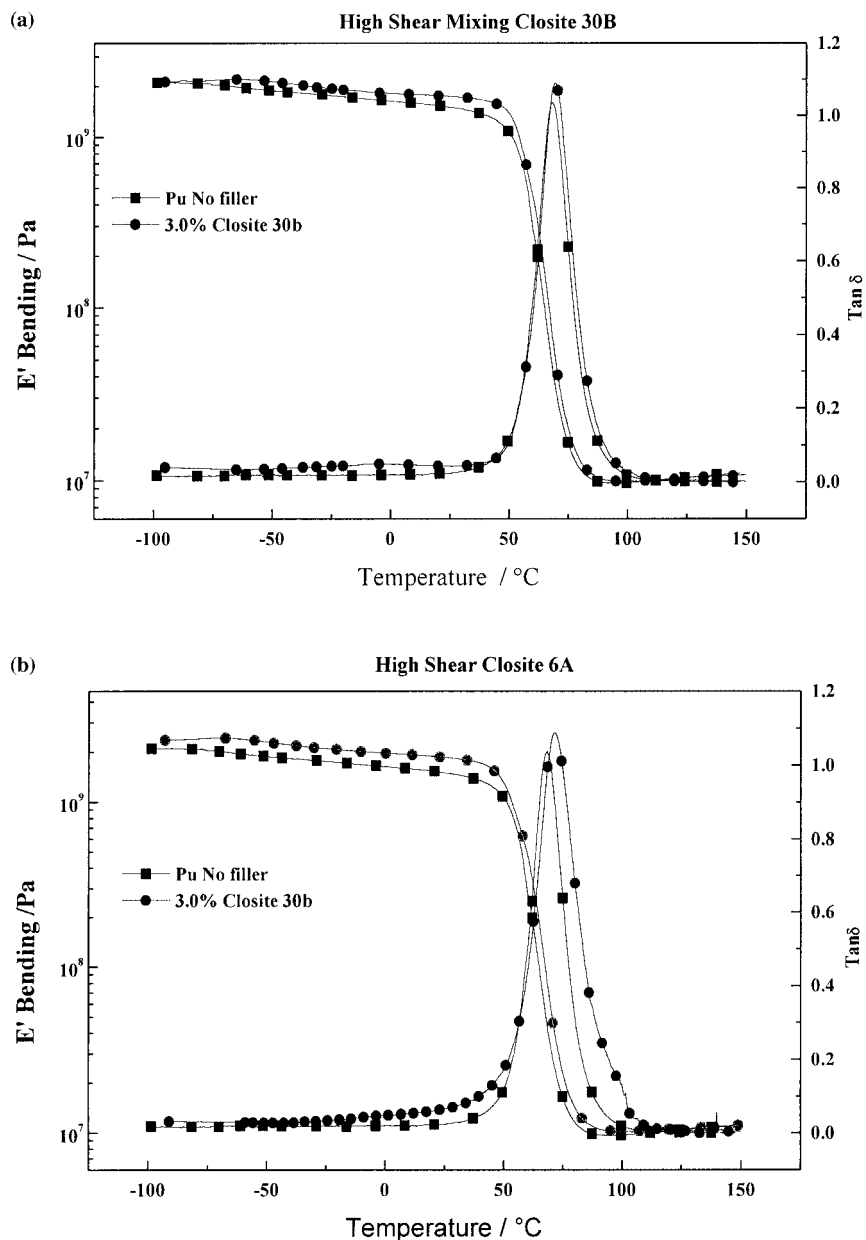


Figure 7 DMTA traces for polyurethanes obtained by high-shear mixing and incorporating (a) unfilled and filler material with 3.0% of Closite 30B and (b) unfilled and filler material with 3.0% of Closite 6 A.

Closite 30B, it is clear that a high degree of exfoliation can be achieved, as indicated by the loss of a definitive scattering peak in the range measured. In contrast, Closite 6A, which shows two peaks in the region studied, exhibits no evidence of exfoliation for the dispersions studied. Viscosity data would suggest that the levels of dispersion of the platelets achieved in the case of Closite 30B are never achieved in the case of Closite 6A.

DMTA data

DMTA traces were obtained for the cured polyurethane materials (Figs. 7 and 8). For both Closite 6A and

Closite 30B nanocomposites below the T_g , there is a marked increase in the modulus even at very low clay loading. At 3% loading, Closite 6A shows an increase of almost 50% in the E' bending modulus and Closite 30B shows a corresponding 30% increase in the E' bending modulus. Examination of the E' bending modulus above the T_g reveals some expected results: In this region, the material is viscoelastic and an increase in the modulus in this region can be attributed to additional interaction being present in comparison with the base polyurethane material and is indicative of chemical interactions between the filler and the polymer chains, creating effective crosslink sites in the matrix. There is a steady increase in the modulus for

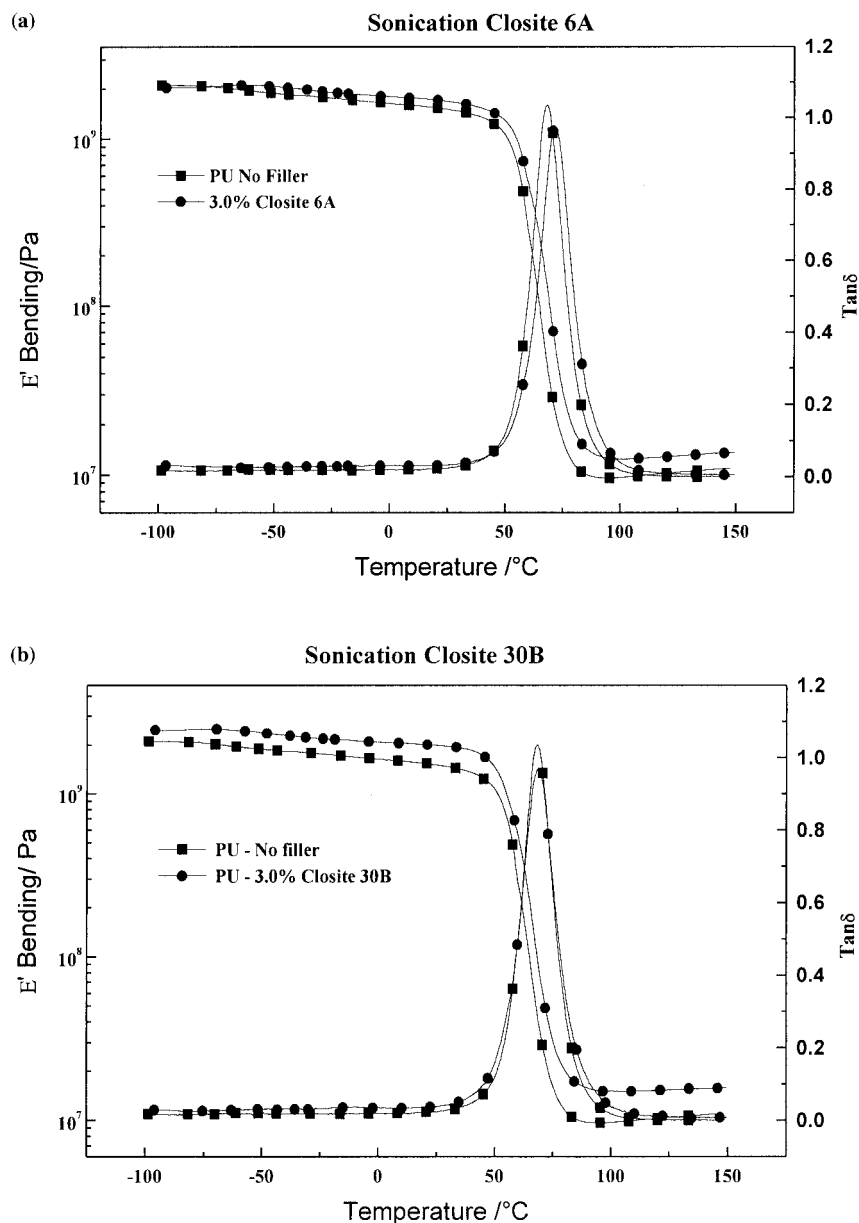


Figure 8 DMTA traces for polyurethanes obtained by sonication and incorporating (a) unfilled and filler material with 3.0% Closite 6A and (b) unfilled and filler material with 3.0% Closite 30B.

both materials going from 0 to 3% filler loading. For Closite 6A, this is almost 30%, and for Closite 30B, a 55% increase in the modulus compared with the unfilled polymer. By comparison, the spread of the results from the T_g analysis are almost within the experimental error and no significant increase was observed.

It appears that the incorporation of the nanocomposite does not lead to an enhancement of the T_g . It is normally assumed that the incorporation of an interacting filler will lead to an increase in the T_g , however, whether or not the T_g increases can depend on a subtle interplay of enthalpic and entropic interactions on the mobility of the soft polyether phase.

Surprisingly, there were no marked differences in the T_g 's of the polyurethanes with the dispersion method. The E' bending modulus of the polyurethanes created with Closite 6A and Closite 30B clays prepared via high shear and their sonicated complements had similar values below the T_g . Above the T_g , however, there were definite differences between the two methods of dispersion for Closite 30B. Whereas sonication promotes a strong increase in the modulus, high shear mixing does not seem to have an effect on the modulus at any loading and presents quite a flat, linear trace characteristic of a noninteracting filled system. The data for the Closite 6A-filled polyurethane, although not quite as obvious, shows a similar

trend with higher values seen for the sonicated materials.

CONCLUSIONS

Both methods of dispersion (high shear and sonication) are able to provide a reinforcing effect, albeit a slight one, to the polymer matrix. Evidence for the reinforcement effect is demonstrated as an increase in the magnitude of the E' bending modulus below the glass transition temperature for both sets of results. High shear mixing, however, does not offer as much clay surface area to the polymer matrix as does the sonication method. This is particularly obvious from a comparison of the E' bending moduli below the T_g for Cloisite 30B. From these observations, it can be concluded that, although there would appear to be platelet-polymer interaction, the effect is very small and is not seen as a dramatic increase in reinforcement of the polymeric material. If there are benefits afforded to sonicated materials, it is only evident above the T_g . It is interesting to note that the enhancement in the viscosity is dependent on the nature of the organic modification being greater in the case of Cloisite 30B in comparison with Cloisite 6A. It would appear that the organic modification not only is able to favor an intercalated state but also reduces the interaction with the polyol.

One of the authors (I. R.) wishes to acknowledge the support of a grant from the EPSRC for the period of this research. The samples of the clays used in this study were donated by Bert Powell and Dave Shaw.

References

1. Komori, Y.; Kuroda, K. In *Polymer-Clay Nanocomposites*; Pinnavia, T. J.; Beall, G. W., Eds.; Wiley: Chichester, New York, 2001; p 3.
2. Vaia, R. A. In *Polymer-Clay Nanocomposites*; Pinnavia, T. J.; Beall, G. W., Eds.; Wiley: Chichester, New York, 2001; p 229.
3. Novak, B. M. *Adv Mater* 1993, 5, 422
4. Giannelis, E. P. *Adv Mater* 1996, 8, 29.
5. Giannelis, E. P.; Krishamoorti, R.; Manias, E. *Adv Polym Sci* 1999, 138 107.
6. Fisher, H. R.; Gielgens, L. H.; Koster, T. P. *Acta Polym* 1999, 50, 122.
7. Zilg, C.; Mulhaupt, R.; Finter, J. *Macromol Chem Phys* 1999, 200, 661.
8. Wang, M. S.; Pinnavai, T. J. *Chem Mater* 1994, 6, 468.
9. Krishamoorti, R.; Vaia, R. A.; Giannelis, E. P. *Chem Mater* 1996, 8, 1728.
10. Choi, H. J.; Kim, S. G.; Hyun, Y. H.; Jhon, M. S. *Macromol Rapid Commun* 2001, 22, 320.
11. Akelah, A.; Moet, A. *J Appl Polym Sci Appl Polym Symp* 1994, 55, 153.
12. Pignon, F.; Magnin, A.; Piau, J.-M.; Cabane, B.; Lindner, P.; Diat, O. *Phys Rev E* 1997, 56, 3281.
13. Hoffman, B.; Dietrich, C.; Thomann, R.; Friedrich, C.; Mulhaupt, R. *Macromol Rapid Commun* 1994, 45, 59.
14. Barnes, H. A. *A Handbook of Elementary Rheology*; Institute of Non Newtonian Fluid Mechanics, University of Wales, 2000.